

Surge arrester allocation for lightning protection of VSC based HVDC prototype

Ali Burhan Haliloglu^{a,b,*}, Ires Iskender^c

^a Department of Energy Technologies, Marmara Research Center (MAM), Scientific and Technological Research Council of Türkiye, Ankara 06800, Türkiye

^b Department of Electrical and Electronics Engineering, Gazi University, Ankara 06560, Türkiye

^c Department of Electrical and Electronics Engineering, Cankaya University, Ankara 06790, Türkiye



ARTICLE INFO

Keywords:

Electrical engineering
Power system protection
VSC-HVDC
Lightning protection
Surge arrester allocation

ABSTRACT

High-voltage direct current (HVDC) systems, based on voltage source converters (VSC), enable asynchronous interconnection of grids with different frequencies and contribute to grid stability by controlling power quickly and precisely. Effective protection of these expensive systems, which must be in continuous operation, increases their lifetime. An overvoltage protection study is needed to ensure the proper protection of HVDC systems that contain multiple devices with varying insulation levels. In this study, lightning protection studies on a prototype VSC-based HVDC (VSC-HVDC) system are explained. In line with this, lightning impulses were modeled and applied to various points in the PSCAD model of the prototype VSC-HVDC, and the response of the system combined with the protection equipment was examined. All stages of protective equipment selection were explained step by step. The suitability of the selected protective equipment was verified based on the simulation results. After running dozens of scenarios, the protection coordination was optimized, and the critical points were determined instead of installing surge arresters at each connection point. In this way, a significant cost benefit was obtained for the investment in protective equipment. Finally, the results of the lightning impulse tests performed to verify the insulation of the VSC-HVDC prototype are reported.

1. Introduction

HVDC systems based on voltage source converters (VSCs) have significant advantages in the grid connection of large-scale renewable energy sources, interconnection between asynchronous AC power systems, and black start [1–4]. HVDC systems consist of devices with different insulation levels and components used to control these devices. Due to the increasing size and complexity of control systems, fault diagnosis in power systems and measures to be taken against possible faults are particularly important [5]. Various faults can occur in an HVDC system, such as AC faults, internal converter faults, and DC faults. Faults can often occur due to insulation failures caused by short circuits, switching operations, and lightning strikes [6,7]. Atmospheric lightning affects the system by generating overvoltages due to direct lightning strikes to the system or back flashover voltages after lightning strikes outside the system. If an HVDC system consists of AC and DC parts, system side, precautions must be taken against overvoltages on both sides [8,9].

In this regard, it is necessary to first analyze the overvoltages that the

HVDC system may be exposed to. Critical overvoltage occurrence points should be determined in the system model. Protection equipment should be selected considering the system operating voltage, equipment insulation voltages, and other parameters. The selected equipment should be placed at appropriate points on the model and verified.

Since there are many devices with different insulation levels in HVDC systems, protection coordination work is required to protect the system from overvoltages that may occur. In order to protect systems from lightning strikes, protective devices should be used at critical points, lightning impulse currents should be directed to the ground and the resulting overvoltages should be reduced [10,11].

Studies on the effects of lightning strikes on transmission lines, High Voltage Alternative Current (HVAC) and HVDC systems are available in the literature [12–18]. These studies focus on modeling details such as shunt reactors at the cable terminal, the presence of surge arresters at system connection points, overhead line geometries, tower base impedance, and corona effects. Ref. [19] provides a comprehensive review of the effects of non-standard lightning impulse voltage on the

* Corresponding author at: Department of Energy Technologies, Marmara Research Center (MAM), Scientific and Technological Research Council of Türkiye, Ankara 06800, Türkiye.

E-mail address: burhan.haliloglu@tubitak.gov.tr (A. Burhan Haliloglu).

insulation of power system equipment. In [20,21], it is pointed out that an overvoltage protection coordination study should be completed before performance tests are performed on HVDC systems. In [21–24], information is given on the determination of surge arresters that should be used for HVDC systems consisting of VSC and Current Source Converter (CSC) based converters. The studies in [25–29] state the necessity of performing submodule, high voltage energization, operation, power quality, performance, partial discharge, and insulation tests before commissioning HVDC systems, and also provide information about these tests. Apart from these, there are also studies on the use of surge arresters in the AC system in VSC-HVDC systems, surge arrester optimization in electrical distribution systems, and the use of metal oxide surge arresters against overvoltages in Line Commutated Converter (LCC) based HVDC systems [30–32]. There are also studies on reducing surge arrester failures caused by direct lightning strikes, determining the parameters of metal-oxide surge arresters, analyzing transient overvoltages on surge arresters in LCC-HVDC systems [32], comparing the circuit structures of metal oxide surge arresters and the electric fields generated around metal oxide surge arresters [33,34].

The main contribution of this study is to develop the most appropriate and analytical approach to determine the critical points where surge arresters can be placed against lightning impulse currents due to atmospheric effects in a VSC based HVDC system. In this context, instead of placing surge arresters at all connection points of the system, the most critical points of a real VSC-HVDC system are determined according to the simulation results, and the number of surge arresters at these points is optimized. The results of the simulation studies on the prototype model and the results used to determine the number and location of surge arresters are given. The determination of the characteristics of the protection devices to be preferred is explained step by step. Then, an optimal protection scheme is developed by evaluating the results of dozens of scenarios applied in this study. In this way, a significant economic advantage is obtained in terms of expenditures on protective devices. Finally, after the simulation and protection device optimization studies, the lightning impulse test results on the VSC-HVDC prototype are presented to verify the insulation.

The Modular Multilevel Converter (MMC) type VSC based HVDC prototype, the subject of this paper, is the first of its kind in Turkey. Mechanical design, control, power stage implementation, and protection software were all done by local engineers.

This paper is organized as follows: Section 2 describes the prototype VSC based HVDC system, followed by details of the modeling studies. The arrester selection procedure is described in Section 3, whereas simulation results are presented in Section 4. Lightning impulse test results are presented in Section 5, followed by discussion and conclusions in Section 6 and 7, respectively.

2. HVDC prototype system

As part of the project, whose main motivation was to develop a VSC-HVDC system with a capacity of 100 MVA (2×50 MVA), a prototype system was designed and implemented. The prototype system consists of self-commutated modular multi-level converters (MMC) with a nominal capacity of 10 MVA. While the voltage level of the main project (real system) is 34.5 kV, the voltage level of the prototype system, which consists of fewer submodules than the real system, is 5.5 kV. In the prototype system, only one transformer was used for grid connection. The input of one converter and the output of the other converter were connected to the output of the 1 MVA test transformer. In this connection, the transformer only provided the power loss of the converters and during the simulations and tests, active/reactive power was circulated between the two converters.

The submodules were designed as half-bridge as shown in Fig. 1 and were connected in series via copper busbars as shown in Fig. 2.

The submodules consist of two semiconductor switches (IGBT₁-D₁, IGBT₂-D₂), a mechanical bypass switch (S), a capacitor (C_{dc}), a discharge

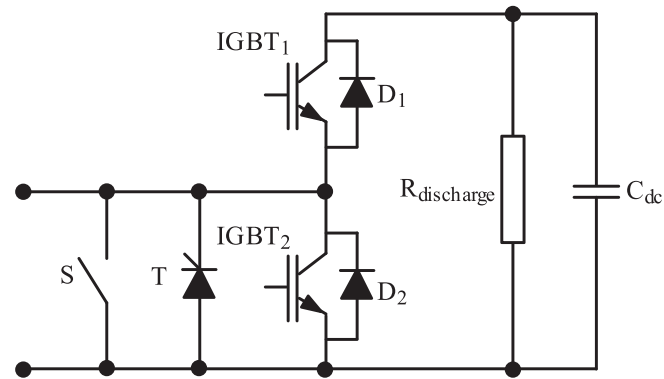


Fig. 1. Half-bridge submodule of prototype system.

resistor (R_{discharge}), and a thyristor bypass switch (T). The prototype system consists of 84 submodules, as can be seen in Fig. 2. In each arm, there are a total of 14 submodules, 7 on the upper arm and 7 on the lower arm per phase.

3. Modeling studies & arrester selection procedure

Simulations performed as part of the overvoltage protection studies for the VSC-HVDC system are included in this section. In the simulations in this study, lightning impulse is used as the overvoltage source for fault analysis. In the prototype VSC-HVDC, the converters are located at the same station and connected to the same busbar in an indoor environment. Since there is no possibility of a direct lightning strike on the DC busbar, the selection of protective devices at the DC side is not considered in this study. In the outdoor environment, there are line and arm reactors, pre-charge resistors, and a coupling transformer. Therefore, the area where the outdoor equipment can be struck by lightning was taken into consideration in the simulation studies. In the simulation studies, lightning strikes were applied to different points of the prototype while at the same time the protection equipment was placed and the response of the system was analyzed.

3.1. HVDC prototype system modeling

The valve structure of the HVDC prototype system is shown in Fig. 3 and as can be seen, submodules are arranged as phases A, B, and C from top to bottom.

The circuit equivalents of submodules, IGBTs, diodes, thyristors and capacitor shown in Fig. 1 were modeled and simulated using PSCAD. The simulations were set with a solution time step of 0.1 μ s to accurately analyze the effects of the lightning impulse waveform, given that the standard lightning impulse signal is 1.2/50 μ s. The lightning strikes applied at t = 0.65 s of the simulation and the system responses can be found in Section 4.

3.2. Lightning impulse modeling

To analyze direct lightning strikes, the lightning channel is usually represented by an equivalent current source that injects current into the system [35,36]. In the literature, there are several functions for representing lightning impulses. The most common of these functions are the double ramp, the double exponential, and the Heidler function [37]. In this study, the double exponential function was used, whose formula is given in Eq. (1).

$$I_{(t)} = kI_0(\exp^{-\alpha t} - \exp^{-\beta t}) \quad (1)$$

Where I₀ is the surge current magnitude, k is the correction factor, α is the negative number specifying time to half value (T₂) and β is the negative number specifying the front time (T₁) of the lightning impulse

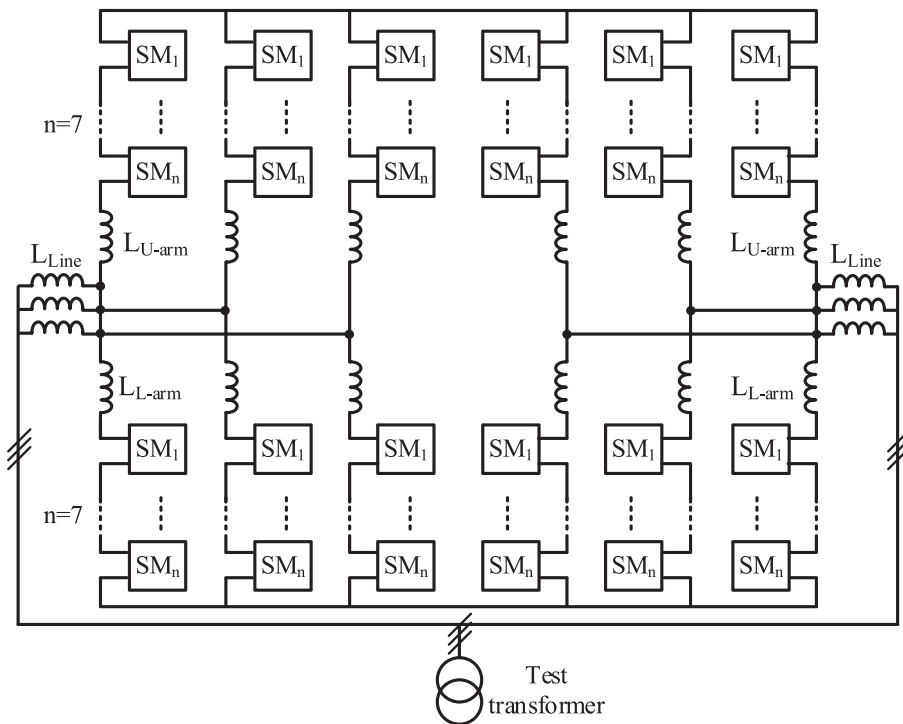


Fig. 2. HVDC prototype system circuit diagram.

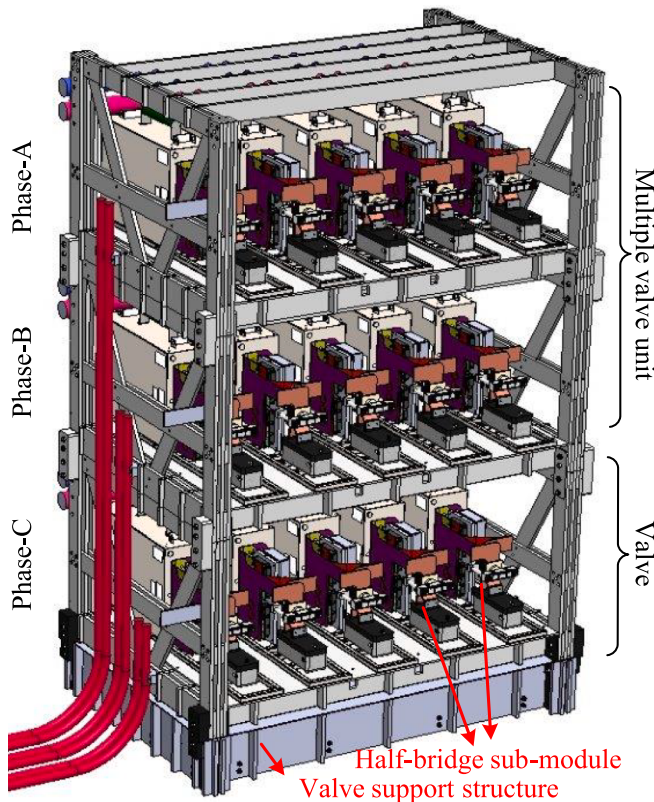


Fig. 3. Valve structure of HVDC prototype system.

waveform [37,38].

According to Eq. (1), the standard waveform whose amplitude is controlled by an external control circuit is shown in Fig. 4. The external control circuit consists of two similar parallel paths with time as a

common input parameter. Each path is multiplied by a factor and expressed as an exponential function. The waveform obtained from the difference of these exponential values is fed to the current source and injected into the system as a current impulse [39].

The overvoltages caused by lightning strikes are characterized by a voltage waveform of $1.2/50 \mu\text{s}$. In the IEC standard [40], which provides recommendations for the selection and application of surge arresters, the lightning current impulse is specified as $8/20 \mu\text{s}$. In [41,42], the average parameters of the lightning current impulse are given as $5.5/77.5 \mu\text{s}$, based on data from Berger. The IEC standard [43], which describes the general principles to be followed to protect structures, equipment, and people from lightning strikes, recommends 2 types of current waves; $10/350 \mu\text{s}$ for direct lightning strikes and $8/20 \mu\text{s}$ for indirect lightning strikes. Consistent with this information, $8/20 \mu\text{s}$, $1.2/20 \mu\text{s}$, $1.2/50 \mu\text{s}$, $5.5/77.5 \mu\text{s}$ and $10/350 \mu\text{s}$ impulses were applied to the system using the lightning impulse generator in Fig. 4 and their effects were investigated. The coefficients in Eq. (1) for generating the applied impulses are given in Table 1.

3.3. Selection of protection equipment

This section describes how the protective equipment and other selected parameters, such as continuous operating voltage of the protective equipment used in modeling studies and the lightning impulse current peak value, are determined. Surge arresters are protective devices used to limit transient overvoltages and divert overcurrents to the ground. The most important feature of surge arresters used as protective devices is that the internal resistance decreases as the voltage difference between the terminals increases [8].

3.3.1. Selection of nominal discharge current

In [41,42], the peak lightning surge current is given as 30 kA based on Berger's data. On the other hand, the standard recommends lightning current ratings of 2.5 kA , 5 kA , 10 kA , or 20 kA for metal oxide surge arresters [44]. For unshielded outdoor equipment, such as busbars, a coordinated lightning peak current of 10 kA (with a waveform of $8/20 \mu\text{s}$) is generally used [45]. Statistical analysis of lightning measurements

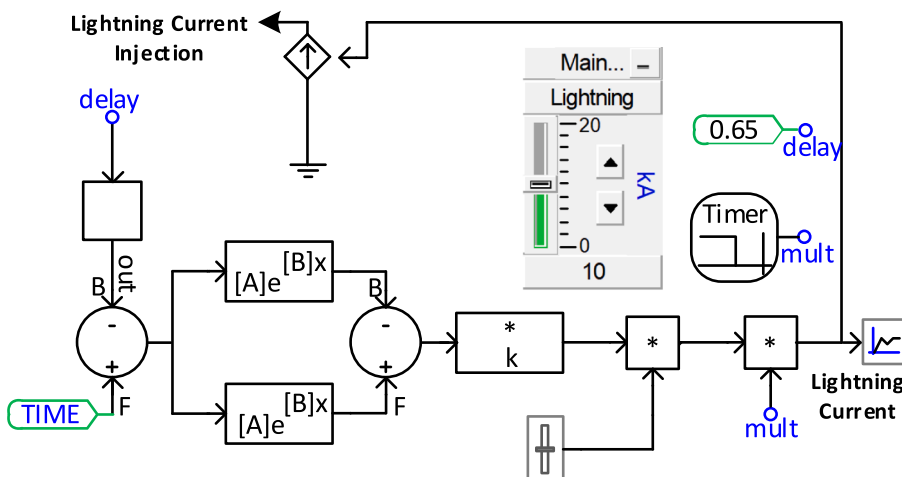


Fig. 4. Lightning impulse generator model.

Table 1
Double exponential function coefficients.

Parameter	k	α	β
8/20 μ s	4	-8.66×10^4	-1.73×10^5
1.2/20 μ s	1.055	-3.99×10^4	-4.22×10^6
1.2/50 μ s	1.02	-1.3×10^4	-4.4×10^6
5.5/77.5 μ s	1.069	-9.9×10^3	-8.1×10^5
10/350 μ s	1.025	-2.05×10^3	-5.64×10^5

in different parts of the world has shown that approximately 90 % of lightning strikes have an amplitude of 10 kA [41].

Ground flash density (N_g) is the number of lightning strikes per square kilometer per year and is often considered the primary descriptor of lightning occurrence in lightning protection studies. Detailed information on this subject can be found in [46]. If the N_g value of the facility to be protected is known, information can be obtained about the peak lightning currents to which surge arresters can be exposed. N_g also contains probability information for lightning peak currents of different magnitudes. According to [46], the ground flash density at the location where VSC-HVDC is installed is 6. Therefore, the probability of a 10 kA amplitude lightning strike is 0.17 per year, or once every 5.8 years.

Consistent with this information, in addition to 10 kA amplitude lightning strikes, 20 kA, 30 kA, 50 kA, and 100 kA lightning strikes were used in the simulations.

3.3.2. Selection of arrester type

Surge arresters are divided into two classes depending on the maximum voltage between the phase and ground (U_s): station class ($U_s \geq 72.5$ kV) and distribution class ($U_s \leq 52$ kV). These classes are also divided into three groups: heavy, medium, and light [44]. Light arresters have the lowest energy capacity among these three distribution classes. Medium arresters are also known as 5 kA arresters, and heavy distribution class arresters are known as 10 kA surge arresters.

Since the voltage level of the prototype system is 5.5 kV, the voltage level of the real system is 36 kV, and the amplitude of the selected lightning impulse current is at least 10 kA, heavy distribution class arresters were preferred in this study. Detailed information on the classification of surge arresters especially for HVDC systems, can be found in [47].

3.3.3. Selection of preliminary continuous operating voltage and rated voltage

The continuous operating voltage (U_c) of an arrester is defined as the specified allowable rms value of the line frequency voltage that can be applied continuously between the arrester terminals. This parameter is

critical for the life of surge arresters, which remain energized for most of their lifetime [20]. According to Eq. (2) the minimum U_c value for the surge arrester should be equal to or 5 % higher than the maximum phase-to-ground voltage (U_s) that can occur during the life of the surge arrester [40]. A safety factor of 5 % is accepted by the industry for applications.

$$U_c \geq U_s / \sqrt{3} \times 1.05 \quad (2)$$

The rated voltage of the arrester (U_r), i.e. the maximum permissible rms value of power-frequency voltage between its terminals at which it should operate properly under the conditions of TOV ($t = 10$ s), is also given in Eq. (3).

$$U_r = U_c \times 1.25 \quad (3)$$

The operating voltage of the prototype of the VSC-HVDC system is 5.5 kV, but the maximum allowable voltage of the transformer (U_s) used is 7.2 kV. If U_s is assumed to be 7.2 kV, then U_c and U_r can be calculated as 4.36 kV and 5.45 kV, respectively, according to Eq. (2) and Eq. (3).

3.3.4. Selection of final continuous operating voltage and rated voltage

Temporary overvoltage (TOV) is a power frequency overvoltage of relatively long duration and the purpose of this step is to test the preliminary U_c for the worst case expected TOV. Since in most cases the overvoltage levels in distribution systems are not precisely known, the situation during a ground fault in the system is considered the worst case. For this reason, the ground fault factor can be used to determine the transient overvoltage rise in the system in fault-free phases. Since it is not possible to calculate this rise completely, it is recommended to multiply the calculated values by the given coefficients, which depend on the grounding conditions of the system. Earth fault factor (k), a value of 1.25 is recommended for four-wire multi-grounded wye systems, 1.4 for three-wire single-grounded systems, and 1.73 for three-wire impedance-grounded systems, delta or isolated systems [40,46]. The HVDC prototype system is connected to the grid with a delta/star transformer, but its secondary is not grounded. For this reason, the earth fault factor was assumed to be 1.73. In line with this information, Eq. (4) was used in the calculations according to the requirements of TOV, in which the earth fault factor is also considered, instead of Eq. (2).

$$U_c \geq (k \times U_s) / (T \times \sqrt{3}) \times 1.05 \quad (4)$$

T is the factor corresponding to 10 s and is given as 1.3 p.u. in the data sheet of the selected surge arrester. In this case, U_c was calculated as 5.81 kV and U_r as 7.27 kV. Finally, a distribution heavy surge arrester with $U_r = 7.5$ kV was selected by rounding the calculated value to the next available standard voltage rating.

3.3.5. Selection of protection level

The protection level (U_{pl}) is the lightning protection level of the arrester (LIPL), i.e., the maximum residual voltage of the arrester (U_{res}) at the rated discharge current. In general, the protection level should be as low as possible to achieve optimum protection. A small protection ratio corresponding to U_{pl}/U_c means that for the same U_c value, the protection level is lower and the protection is better. If it is technically necessary to use a very low protection level, it is possible to choose an arrester with a better protection rate [48]. Surge arresters with a better protection rate consist of larger diameter metal-oxide resistors and therefore have a higher energy transfer potential. Therefore, U_{pl}/U_c , protection ratio, rated discharge current, and energy transfer capacity should also be taken into consideration when selecting a surge arrester or comparing products of different brands.

The U_{pl} value of the surge arrester must be lower than the lightning impulse withstand voltage (LIWV) of the equipment to be protected. On the other hand, the surge arrester to be selected is exposed to all voltage stresses occurring in the system as well as lightning strikes. For this reason, it is recommended to select the U_c value slightly higher than the highest voltage value of the system U_s or U_{TOV} value [48].

It is recommended to use a protection factor (K_s) between the LIWV of the devices used in the system and the maximum value of the lightning surge. This protection factor takes into account the aging of the insulation of the devices and the statistical uncertainties in the definition of the LIWV. It is recommended to set K_s to 1.15 for outdoor insulation [49].

3.3.6. Selection of protection equipment locations

The protection scheme of the VSC-HVDC prototype system is shown in Fig. 5. R_{Prec} in Fig. 5 is the pre-charge resistor, L_{Line} is the line reactor, L_{U-arm} and L_{L-arm} are the upper and lower arm reactors, respectively. Since the VSC-HVDC prototype system was built in a back-to-back structure, both converters were located in the same station, and the connection between them was made on the DC side by copper busbars shown in Fig. 5 with dashed black lines.

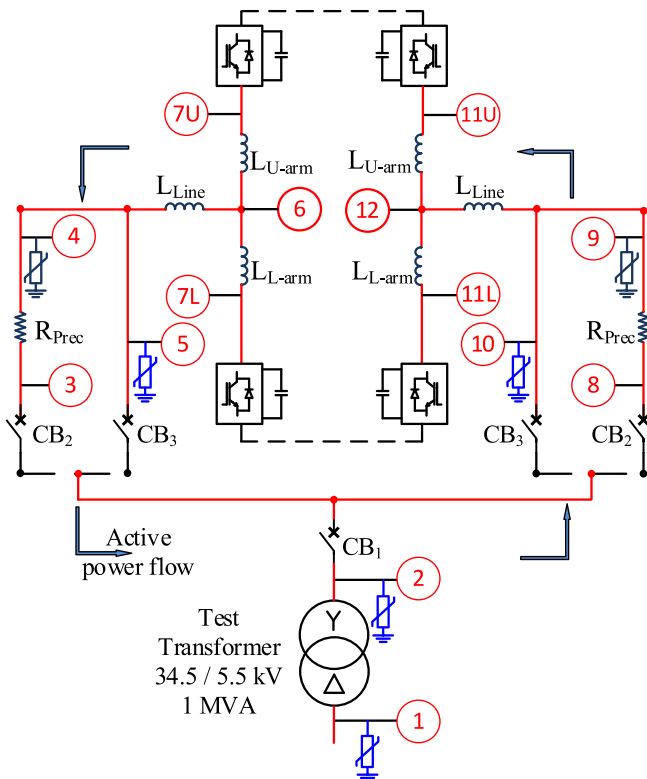


Fig. 5. Protection scheme of VSC-HVDC prototype.

Table 2

Selected surge arresters and their characteristics.

Location in Fig. 5	U_c (kV)	U_r (kV)	Selected U_r	LIWV (kV)	U_{pl} (kV)	LIWV/ U_{pl} Margin	U_{pl}/U_c
1	31.38	39.22	37.5	170	105	1.62	3.35
2-12	5.8	7.26	7.5	60	21	2.86	3.62

In addition, the medium voltage cables, which are located outdoors and may be exposed to lightning strikes, are shown with solid red lines in Fig. 5. The prototype VSC-HVDC system was operated as a closed loop by connecting the converters of the prototype system to the same AC busbar.

The locations in the remainder of this study refer to locations ① through ⑫ marked in Fig. 5. In the simulation studies, lightning strikes were performed at the locations numbered ① to ⑫ in Fig. 5 under various scenarios. When lightning strikes were applied, the voltage and current waveforms at the numbered locations were observed separately with single protective equipment, multiple protective equipment, or without any protective equipment.

The surge arresters selected based on the calculations performed in Section 3.3 are used in the simulations for the system shown in Fig. 5, and their characteristics are listed in Table 2. In Table 2, the voltage levels on the secondary side of the transformer are the same for locations ② to ⑫ in Fig. 5, and the surge arresters selected for this side have the same characteristics.

4. Simulation results

In the simulations, 8/20 μ s, 1.2/20 μ s, 1.2/50 μ s, 5.5/77.5 μ s, 10/350 μ s waveforms with 10 kA, 20 kA, 30 kA, 50 kA, 100 kA amplitudes were applied to the system in different scenarios. However, for clarity, only the results of different waveforms with a 30 kA amplitude are given in the figures below, while the results of all amplitudes are given in the Table 3 and Table 4. Parameters such as the currents flowing through the arresters, the currents in the system, the voltages of the arresters, the thermal charge value transferred from the arresters, and the operational performance of the system after lightning strikes of different amplitudes and waveforms were monitored. The results of each scenario were studied and the optimal protection configuration with surge arresters was determined.

Since it is not possible to include all the figures of the simulation results and this is the first point where the effects of lightning strikes that may hit the grid side, the lightning strikes applied to location ② are based on the simulations.

4.1. Presence of a surge arrester at the location of the lightning strike

In this scenario, when lightning strikes were applied at different points, it was observed that there was only one surge arrester at the point where the lightning was applied. However, for clarity of the figures, simulation results with a 30 kA amplitude are only given for location ②. Simulation results that include lightning impulses with other amplitudes can be found in Section 4.4.

The applied lightning impulse currents of 30 kA amplitude are shown in Fig. 6 and the arrester voltages at the time of application are shown in Fig. 7. The U_{res} value of the selected arrester is 21 kV and Fig. 7 shows that the maximum value is about 15 kV, which confirms that the selected surge arrester is suitable. It was also observed that all lightning impulse currents with an amplitude of 30 kA are discharged through the surge arrester when a surge arrester is present at the location of lightning strike.

The thermal charge values transferred to the ground by the arrester during lightning strikes with an amplitude of 30 kA are shown in Fig. 8. Depending on the type of lightning strike shown in Fig. 6, the thermal

Table 3

The effect of using parallel surge arresters.

Lightning impulse	Number of arresters at location ②	Thermal charge value at an impulse magnitude of				
		10 kA	20 kA	30 kA	50 kA	100 kA
8/20 μs	Single	0.454	0.928	1.422	2.467	5.422
	Two parallel	0.445	0.905	1.375	2.342	4.931
1.2/20 μs	Single	0.510	1.040	1.588	8.913	30.611
	Two parallel	0.499	1.017	1.543	2.621	19.250
1.2/50 μs	Single	1.516	3.098	4.730	14.419	42.652
	Two parallel	1.485	3.030	4.599	7.813	30.285
5.5/77.5 μs	Single	1.689	3.678	5.774	10.216	22.630
	Two parallel	1.666	3.614	5.644	9.847	21.085
10/350 μs	Single	9.639	19.711	30.103	51.851	111.840
	Two parallel	9.445	19.277	29.268	49.733	103.702

Table 4

The effect of using surge arresters at different locations.

Lightning impulse	Q _{arrester}	Thermal charge value at an impulse magnitude of				
		10 kA	20 kA	30 kA	50 kA	100 kA
8/20 μs	②	0.170	0.393	0.611	1.055	2.240
	③	0.138	0.264	0.393	0.655	1.340
	⑩	0.135	0.245	0.362	0.601	1.225
1.2/20 μs	②	0.181	0.422	0.667	1.166	2.457
	⑤	0.159	0.304	0.452	0.749	1.505
	⑩	0.156	0.287	0.421	0.692	1.377
1.2/50 μs	②	0.533	1.247	1.972	3.450	7.315
	③	0.471	0.904	1.340	2.222	4.490
	⑩	0.463	0.855	1.252	2.056	4.106
5.5/77.5 μs	②	0.731	1.705	2.689	4.702	9.993
	⑤	0.640	1.229	1.822	3.023	6.118
	⑩	0.629	1.159	1.697	2.790	5.624
10/350 μs	②	3.384	7.916	12.511	21.903	46.571
	③	2.984	5.725	8.488	14.086	28.521
	⑩	2.937	5.426	7.945	13.048	26.190

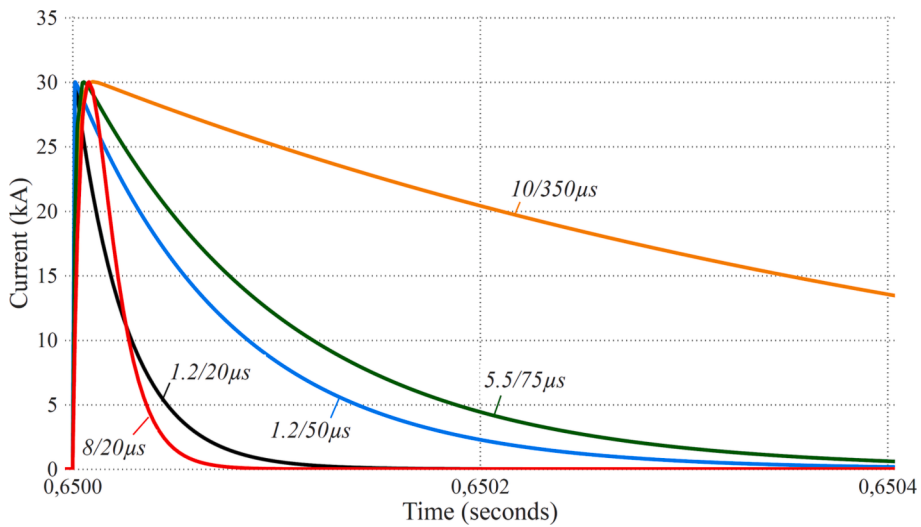
charge values vary between 1.42 C and 29.82 C. However, the upper limit for the thermal charge transfer of the selected surge arrester, whose selection method was explained in [Section 3.3](#), is 1.1 C. In this case, despite having a surge arrester at the point where the lightning strikes, the system was clearly unprotected in the event of a lightning strike with an amplitude of 30 kA. If this situation had happened in reality, the surge arrester would not have been able to fulfill its duty and would have become unusable again. Therefore, it was aimed at reducing the thermal charge value generated by the lightning strike below 1.1 Coulomb.

4.2. Presence of surge arresters at different locations

Since a single surge arrester was not sufficient in the previous scenario, additional surge arresters were placed at ③ and ⑩ in addition to ②, and an 8/20 μs impulse with an amplitude of 30 kA was applied. The distribution of the lightning impulse current to the surge arresters in this scenario is shown in [Fig. 9](#). $I_{arrestertotal}$ in [Fig. 9](#) is the arrester current that occurs when an arrester was present at location ②. As can be seen, a total of 30 kA lightning impulse current flowed from the surge arrester to the ground. Simulation results with waveforms other than 8/20 μs can be found in [Section 4.4](#).

While arresters were present at locations ②, ③, and ⑩, a 30 kA lightning impulse at location ② resulted in the following peak currents flowing through the arresters to the ground: 13.839 kA for location ②, 8.458 kA for location ③, and 7.702 kA for location ⑩. It was found that most of the lightning impulse current flowed through arrester ② into the ground, and the remaining part was unevenly distributed between ③ and ⑩. The reason for this imbalance is the impedance difference between the two sides of the single line diagram in [Fig. 5](#). This impedance imbalance on both sides of the system is due to reasons such as cable lengths and inequalities in the production of the devices. It was observed that the lightning impulse followed a path inversely proportional to the impedance.

In the same scenario, thermal charge transfer (Q_{th}) values from surge arresters are shown in Coulombs (C) in [Fig. 10](#). Q_{th} indicates the ability of distribution type surge arresters to withstand the energy generated by lightning strikes flowing through the surge arresters to the ground. In other words, the most important thing in surge protection is not the actual energy the surge arrester transfers, but the current or load it can withstand during an event without being damaged [\[44\]](#). It was found that the thermal charge transfer of the 8/20 μs impulse with an amplitude of 30 kA was 1.43 C ($Q_{arrestertotal}$) when there was a surge arrester at location ② only. In the presence of surge arresters at locations ②, ③, and ⑩, the thermal charge transfer values for a 30 kA 8/20 μs lightning

**Fig. 6.** Different lightning impulse waveforms applied in simulations.

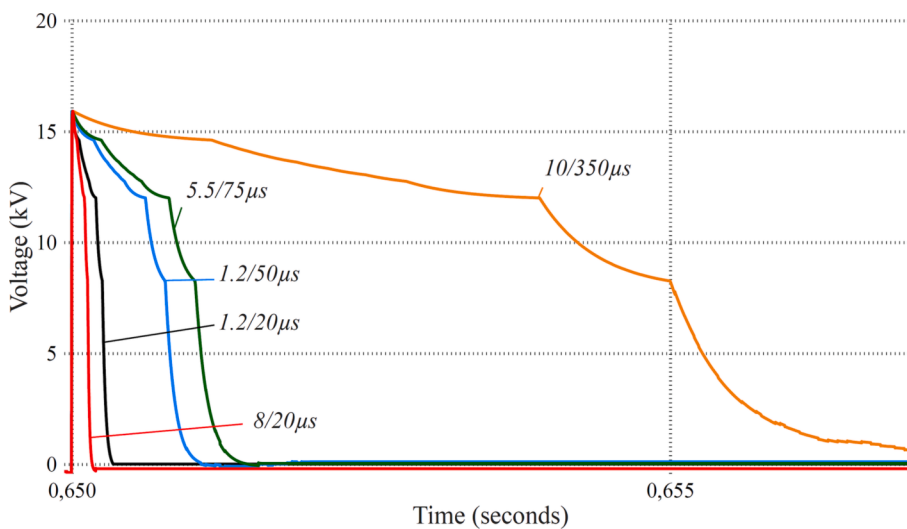


Fig. 7. Arrester voltages at location ② according to different impulse waveforms.

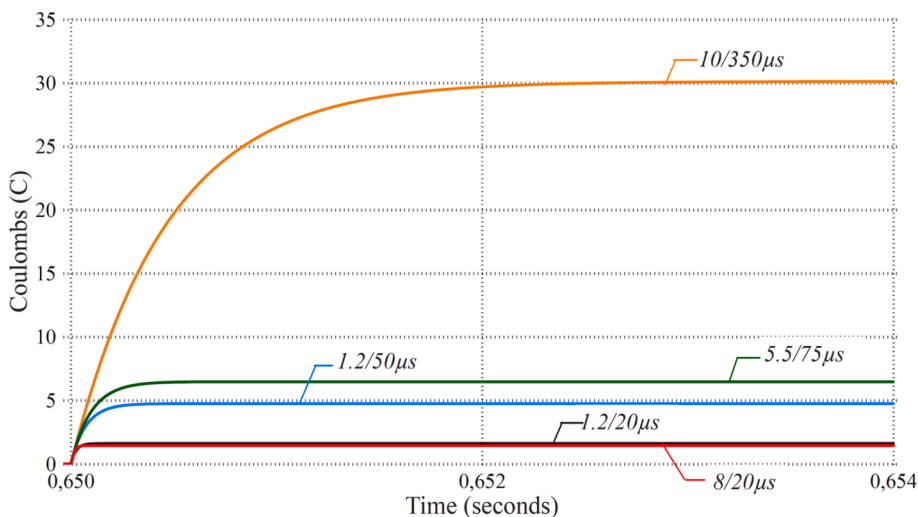


Fig. 8. Arrester thermal charge values at location ② according to different impulse waveforms.

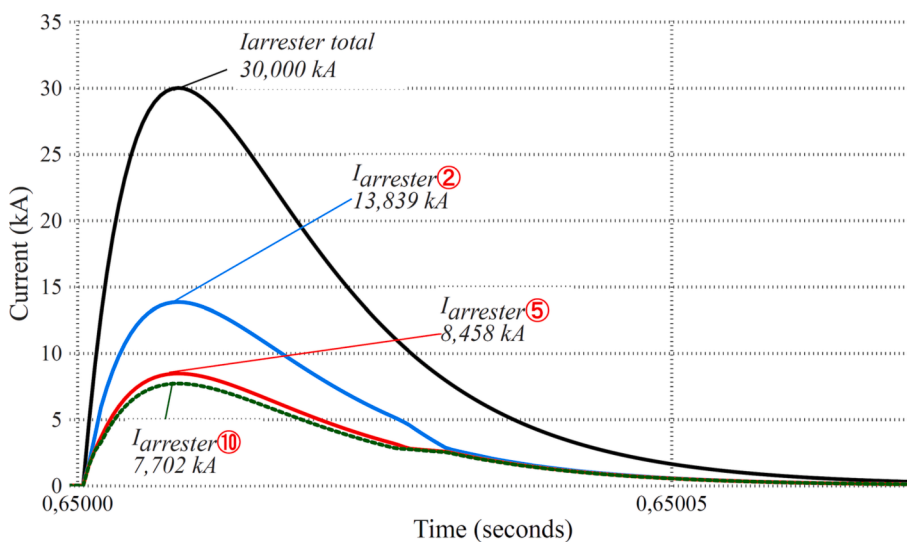


Fig. 9. Distribution of arrester currents between locations ②, ⑤ and ⑩ in the event of a lightning strike (8/20 μs, 30 kA).

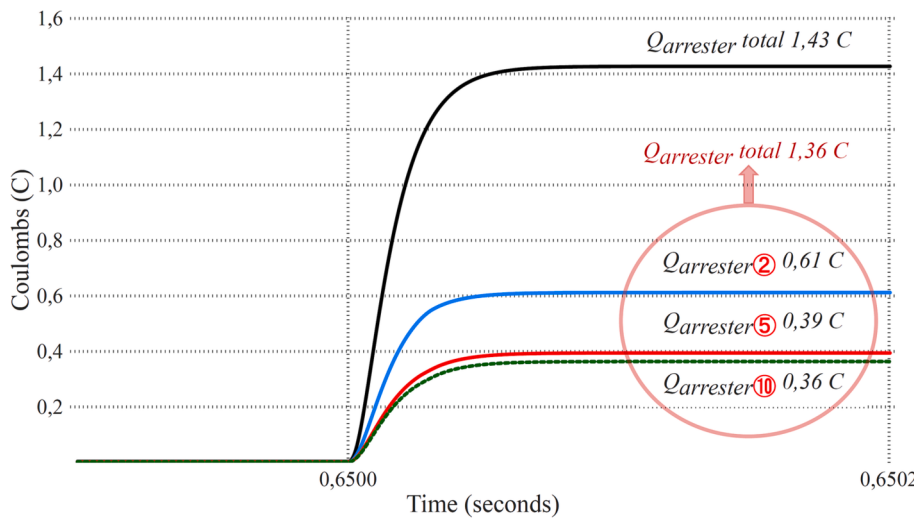


Fig. 10. Thermal charge transfer values of arresters at locations ②, ⑤ and ⑩ in the event of a lightning strike(8/20 μ s,30kA).

impulse at location ② were as follows: 0.61 C for location ②, 0.39 C for location ⑤, and 0.36 C for location ⑩. The unequal sharing of the thermal charge values of surge arresters ⑤ and ⑩ is due to the current sharing corresponding to the impedance difference of the system circuit.

When the surge arresters were placed at locations ②, ⑤, and ⑩, the total thermal charge value of 1.36 C of the surge arrester at location ② was lower than the value of 1.43 C that results when a single surge arrester was placed at location ②. This difference in thermal charge values despite the same lightning impulse was due to the faster transfer of the current impulse to the ground when surge arresters were placed at multiple locations.

4.3. Presence of parallel surge arresters at the same location

Fig. 11 and **Fig. 12** are prepared considering the results of the scenario with a single arrester or two parallel arresters at location ② and the presence of arresters at different locations. **Fig. 11** and **Fig. 12** were plotted considering the simulation results with only 30 kA and 8/20 μ s lightning impulses. Simulation results analyzed with other amplitudes and waveforms are shown in the following tables.

The currents of the arresters at location ② are shown in **Fig. 11** and the values of the thermal charge transfer are shown in **Fig. 12**.

It was observed that when two parallel arresters were placed at the same location and a 30 kA lightning impulse was applied, a current of 15 kA flowed through both surge arresters to the ground. It was also observed in **Fig. 11** that the lightning impulse current was transferred to ground in a shorter time compared to the scenario with a single arrester. For parallel surge arresters, it can also be seen in **Fig. 12** that the thermal charge value per surge arrester decreases from 1.43 C to 0.69 C compared to the single surge arrester scenario. When more than one surge arrester was used, it was observed that the thermal charge value per surge arrester decreased to 0.61 C and 0.46 C, respectively.

4.4. Comparison of scenarios

Table 3 and **Table 4** were prepared according to the results of the scenarios consisting of different lightning impulses applied to the location ②. All values in the tables, starting with **Table 3** up to **Table 7**, show the value of thermal charge transferred to the ground in coulombs (C) per surge arrester in each scenario. Since the upper limit of the thermal charge value of the selected surge arrester is 1.1 C (2.2 C for two parallel arresters), values below this value are accordingly highlighted in green in the tables. Scenario results highlighted in red indicate non-compliant values in the tables.

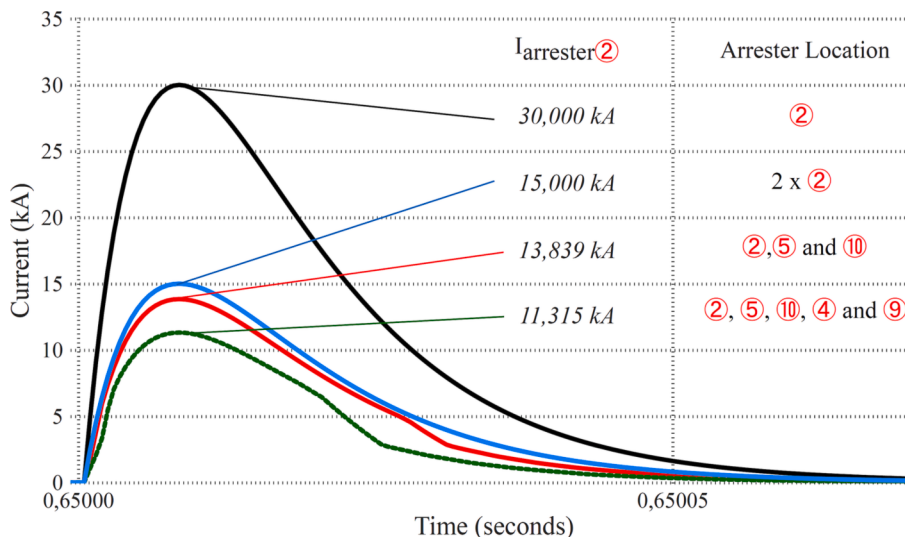


Fig. 11. Arrester currents at location ② in case of lightning strike under different arrester configurations (8/20 μ s, 30kA).

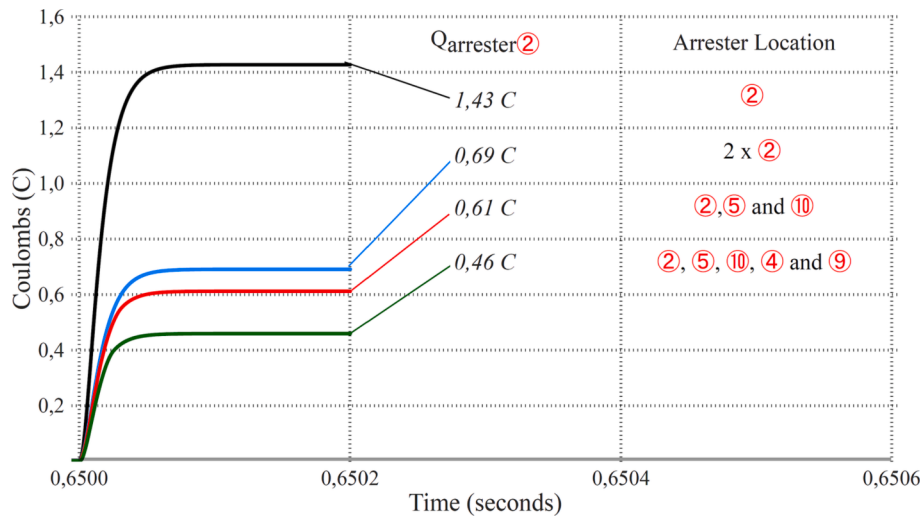


Fig. 12. Arrester thermal charge transfer values at location ② in case of lightning strike under different arrester configurations (8/20 μ s, 30kA).

According to the data in Table 3, installing a surge arrester only at location ② provided adequate protection for some low amplitude lightning strikes (e.g., 8/20 μ s, @ 10 kA or 20 kA). In some cases where one surge arrester was not sufficient, installing a second arrester in parallel provided adequate protection (e.g., 1.2/50 μ s, @ 10 kA). The use of parallel surge arresters in the same location was found to provide an advantage of between 1.4 % and 9 % over the lightning strike variant in terms of the value of thermal charge transferred to the ground. However, in some cases even the addition of a parallel surge arrester did not provide adequate protection conditions. Therefore, scenarios where surge arresters were added at various locations were analyzed. Table 4 was created based on the results of the scenario where, unlike Table 3, surge arresters were used at different locations instead of at the same location. Since locations ②, ⑤, and ⑩ contributed most positively to the protection performance based on the results of the simulations, these values are listed in the table as examples.

Comparing Table 3 and Table 4 for the same type of lightning strikes, it was seen that the scenarios in Table 4 provide more effective protection. According to Table 3, when a parallel surge arrester was installed at location ②, adequate protection was found for a maximum surge of 30 kA at 8/20 μ s. On the other hand, according to Table 4, when surge arresters were installed at locations ②, ⑤, and ⑩, effective protection was found to be provided even for an amplitude of 50 kA at an impulse of 8/20 μ s.

4.5. Surge arrester location optimization

Table 5 summarizes the surge arrester location optimization that emerged after dozens of scenarios consisting of 3 surge arresters at location ② and one each at locations ⑤, ⑩, ④, and ⑨.

Although it is stated in Section 3.3.1 that the probability of a 10 kA lightning strike at the prototype system site is very low, when optimizing

the placement of surge arresters, the aim was to protect against lightning strikes of 5–10 kA amplitude. Table 5 shows that the resulting surge arrester configuration protects which lightning impulse waveform up to how many amps. Consistent with this information, effective protection was determined according to the placement of surge arresters in Table 5 as follows: 8/20 μ s impulse up to 118kA, 1.2/20 μ s impulse up to 108kA, 1.2/50 μ s impulse up to 40kA, 5.5/77.5 μ s impulse up to 30kA, and 10/350 μ s impulse up to 8kA.

The CB₂s in Fig. 13 are the breakers that allow the use of pre-charge resistors during the initial energization of the HVDC prototype. The opening and closing maneuvers of the breakers when energizing the prototype system are shown in Table 6.

During the pre-charging process, i.e., during the 2nd maneuver in Table 6, if lightning comes from the grid while surge arresters are present at locations ④ and ⑨, the lightning impulse current flows through the pre-charging resistors. Therefore, the pre-charge resistors are

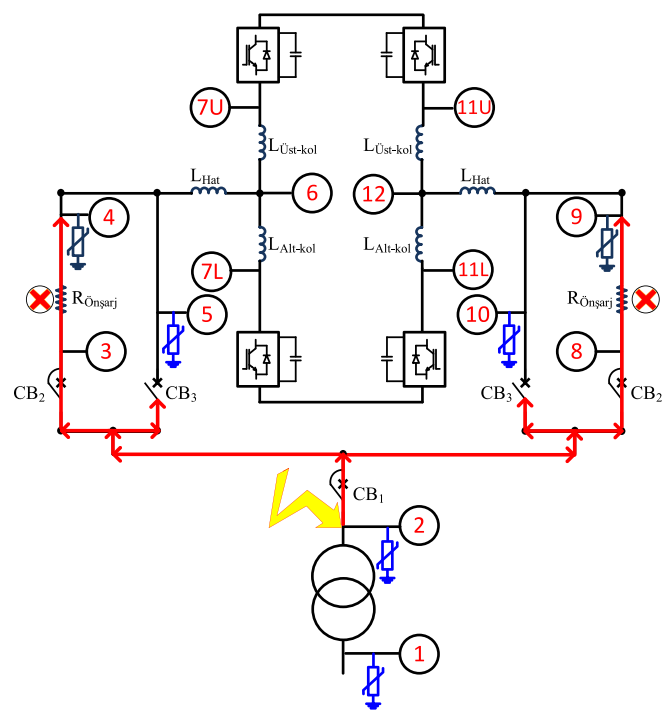


Fig. 13. Single line diagram during pre-charging process.

Table 5
Surge arrester placement optimization of VSC-HVDC prototype.

Lightning impulse	Qarrester	8/20	1.2/20	1.2/50	5.5/77.5 μ s	10/350
		μ s	μ s	μ s	μ s	μ s
3	②	1.084	1.089	1.053	1.016	1.056
1	⑤	0.589	0.623	0.727	0.765	0.992
1	⑩	0.511	0.554	0.686	0.740	0.975
1	④	0.589	0.623	0.727	0.763	0.992
1	⑨	0.511	0.554	0.686	0.739	0.975

Table 6
Circuit breaker maneuvers during energizing.

Process	Maneuver	CB ₁	CB ₂	CB ₃
Start	1st	Close	Open	Open
Pre-charging	2nd	Close	Close	Open
Energization	3rd	Open	Open	Close

damaged. To prevent this damage, surge arresters should be installed at points ③ and ⑧.

After pre-charging process, i.e., during the 3rd maneuver in **Table 6**, if lightning strikes from the grid and surge arrestors are installed at locations ③ and ⑧ instead of locations ④ and ⑨, the lightning current flows through routes ②, ④, ③ or ②, ⑨, ⑧, respectively. Therefore, the pre-charge resistors are damaged.

Consistent with this information, while **Table 5** is the result of positioning surge arresters to provide the most effective protection, an alternative study was required. If precautions are not taken against lightning strikes that may occur during the pre-charging process, which takes approximately 2 min, surge arresters may not be installed at points ③, ⑧, ④, ⑨. In this case, the required positioning of surge arresters for effective protection is given in **Table 7**. **Table 7** summarizes that the optimal surge arrester placement for the prototype VSC-HVDC consists of 3 surge arresters at location ② and one arrester each at locations ⑤ and ⑩.

Consistent with this information, effective protection was determined according to the placement of surge arresters in **Table 7** as follows: 8/20 μ s impulse up to 104 kA, 1.2/20 μ s impulse up to 94 kA, 1.2/50 μ s impulse up to 30 kA, 5.5/77.5 μ s impulse up to 25 kA, and 10/350 μ s impulse up to 6 kA.

5. Lightning impulse test results

The results of lightning impulse tests to confirm the insulation of the prototype VSC-HVDC against lightning strikes are also presented under this heading in addition to optimizing the placement of the surge arresters. Standard lightning impulse waveform is given in **Fig. 14**.

Standard lightning impulse time parameters T_1 and T_2 should be calculated as in Eq. (5) and Eq. (6), respectively [50].

$$T_1 = 1.67(t_{90} - t_{30}) \quad (5)$$

$$T_2 = (t_{50} - t_0) \quad (6)$$

According to the standard [51], lightning impulse test voltage U_{lim} should be determined in accordance with the Eq. (7) for the tests.

$$U_{\text{lim}} = \pm LIP_m \cdot k_8 \cdot k_t \quad (7)$$

LIP_m is the lightning impulse protective level determined by insulation co-ordination, taking into account the arresters connected between the valves high voltage terminal and earth. k_8 is the test safety factor and it is recommended to take 1.1, and k_t is the atmospheric correction factor.

Although the prototype VSC-HVDC system was designed for 5.5 kV, the final system was designed for 36 kV. At a voltage of 36 kV, the peak value of the standard lightning impulse withstand voltage is 170 kV

Table 7
Final lightning protection optimization of VSC-HVDC prototype.

Lightning Impulse	Q _{arrester}	8/20	1.2/20	1.2/50	5.5/	10/350
		μ s	μ s	μ s	77.5 μ s	μ s
3	②	1.099	1.097	0.972	1.087	1.081
1	⑤	0.804	0.850	0.808	0.923	1.054
1	⑩	0.738	0.757	0.768	0.884	1.039

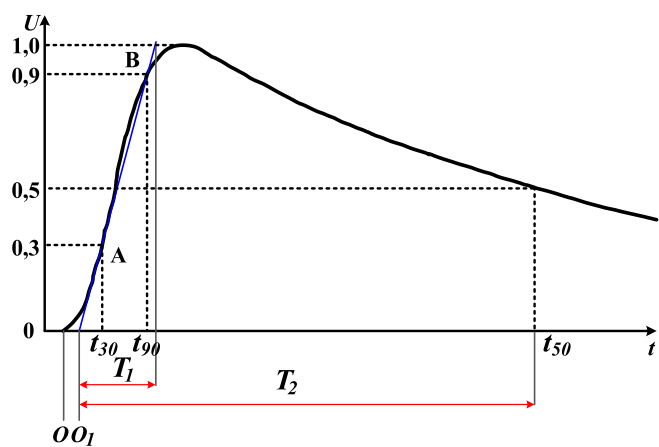


Fig. 14. Standard lightning impulse parameters [11].

[52]. Since the value of 170 kV is greater than the value to be found according to Eq. (7), the lightning impulse test amplitude was set to 170 kV. According to the standard [51] that defines the electrical tests in VSC-HVDC systems, the lightning impulse test consists of three positive polarity impulses and three negative polarity impulses. In addition, the limits for passing lightning impulse tests are given in **Table 8**. If the results obtained after applying positive and negative lightning strikes to the system are within the range shown in **Table 8**, the test results are considered successful [8].

A 200 kV, 10 kJoule high voltage impulse generator, an impulse voltage divider, as shown in **Fig. 15**, and a measurement system, were used for the lightning impulse tests.

A standard positive and negative lightning impulse voltage waveform (1.2/50 μ s) was applied to the system. Details of the 1.2/50 μ s lightning impulse waveform applied to VSC-HVDC can be found in [50,53]. The applied lightning impulse voltages were measured using a high voltage divider and recorded with an oscilloscope.

Fig. 16 shows the oscilloscope recording of the first positive lightning impulse applied between phase B and earth as an example.

As can be seen in **Fig. 16**, $|X_1-X_2|$, $|X_3-X_4|$ and $|Y_1-Y_2|$ values are given. The division ratio of the high voltage divider is 1/1321. Based on this information, V_p , T_1 and T_2 can be calculated as follows.

$$V_p = |Y_1 - Y_2| = 130.4V$$

$$V_p = 130.4 \times 1321 \Rightarrow 172.258kV$$

$$T_1 = |X_3 - X_4| = 780ns$$

$$T_1 = 0.78 \times 1.67 \Rightarrow 1.3026\mu s$$

$$T_2 = |X_1 - X_2| \Rightarrow 50.2\mu s$$

According to these calculated values, the test result can be said to be successful. **Table 9** was formed from other calculated T_1 , T_2 and V_p values by examining the recorded lightning strike graphs. The lightning impulse tests were applied to the system in four different scenarios: Phase-Earth Positive, Phase-Earth Negative, Phase-Phase Positive, and Phase-Phase Negative. An example of a test result from each scenario was shown in **Table 9**.

As can be seen from **Table 9**, all lightning impulse tests performed with the prototype VSC-HVDC system passed within the test passing

Table 8
Lightning impulse test passing criteria.

Parameter	Lightning Impulse	Passing criteria
Test voltage (V_p)	$V_p = 170 \text{ kV} \pm 3 \%$	$164.9 \text{ kV} \leq V_p \leq 175.1 \text{ kV}$
Front time (T_1)	$1.2 \mu s \pm 30 \%$	$0.84 \mu s \leq T_1 \leq 1.56 \mu s$
Time to half value (T_2)	$50 \mu s \pm 20 \%$	$40 \mu s \leq T_2 \leq 60 \mu s$



Fig. 15. High voltage impulse generator.

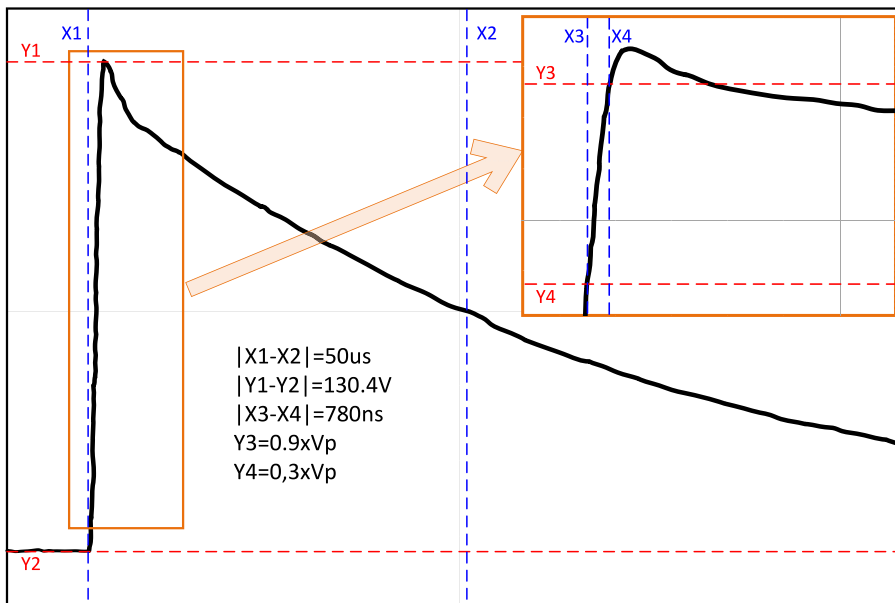


Fig. 16. Phase B to earth positive lightning impulse test result.

criteria given in Table 8. In this case, the insulation of the prototype VSC-HVDC was verified against possible lightning strikes.

6. Discussion

This research focuses on establishing a framework for strategically placing surge arresters to protect VSC-based HVDC prototype from lightning-induced overvoltages. Accordingly, the lightning strokes modeled in PSCAD were applied to the VSC-HVDC prototype system model designed for 5.5 kV. Simulation results showed that it is not useful and economical to install surge arresters at randomly selected locations or at all connection points to protect the entire system. The whole system was evaluated, considering the critical equipment, and the selection of protection devices was verified by simulations.

The most important parameter in surge arrester selection is U_c . The U_c value of the surge arrester should be sufficiently higher than the

voltage between the phase and the ground of the system. The U_{pl} value of the surge arrester should be significantly lower than the LIWV value of the equipment to be protected.

The study revealed that damage from lightning strikes increases with the strength and shape of the lightning. It is crucial to take specific protection measures for each HVDC system, taking into account its specific characteristics and vulnerabilities.

Furthermore, placing multiple surge arresters at specific points in the system helps to distribute the thermal charge more effectively. With this strategy, the time required for the lightning impulse current to reach the ground is shortened, reducing the risk of overloading the single surge arrester and reducing potential damage.

This study also showed that the lightning impulse current travels through the system in a manner proportional to the system impedance.

Table 9
Lightning impulse test results.

Test Point	Polarity	T ₁ (μs)	T ₂ (μs)	V _p (kV)	Results
Phase A to Phase B	+	1.3360	50.4208	172.787	✓
	-	1.3026	48.3708	171.202	✓
Phase B to Phase C	+	1.3026	50.4708	171.202	✓
	-	1.3694	51.0508	173.579	✓
Phase C to Phase A	+	1.3026	49.0508	172.523	✓
	-	1.3360	48.7608	174.901	✓
Phase A to Earth	+	1.4028	54.1408	170.409	✓
	-	1.4696	52.2409	170.409	✓
Phase B to Earth	+	1.3026	50.2004	172.258	✓
	-	1.3026	51.1908	173.579	✓
Phase C to Earth	+	1.3026	48.7508	172.258	✓
	-	1.3026	48.5908	174.636	✓

7. Conclusions

In conclusion, this research addresses the strategic placement of surge arresters in a VSC-based HVDC system. Instead of relying on a uniform placement strategy, the approach of the study enables the identification of critical areas that require surge arresters. The selection of surge arresters for suitable locations is an important task that must be completed before the system is commissioned.

This research highlights the importance of surge arrester optimization, distributed placement, and consideration of impedance imbalances within the system, as well as the direct relationship between the extent of damage caused by lightning strikes and the characteristics of the lightning current.

The optimized approach not only improves the effectiveness of lightning protection, as detailed in this study, but also provides significant cost savings in the field of protection equipment for HVDC systems. In an environment where both reliability and economic efficiency are paramount, these findings carry significant weight and will contribute to future research and practical applications in HVDC systems. Furthermore, specific protection mechanisms should be considered by evaluating the unique characteristics of each HVDC system.

Declaration of Competing Interest

The authors declare that they have no known competing financial interests or personal relationships that could have appeared to influence the work reported in this paper.

Acknowledgments

This research work is carried out within the scope of the research and development of back to back connected MMC type VSC-HVDC system which is funded by TUBITAK Public Research Grant Committee (KAMAG – Project No: 113G008), customized by TEIAS and being directed by TUBITAK MAM (Project No: 5142805). The authors would like to thank these institutions for their support.

References

- [1] N. Flourentzou, V.G. Agelidis, G.D. Demetriadis, VSC-Based HVDC Power Transmission Systems: An Overview, *IEEE Trans. Power Electron.* 24 (2009) 592–602, <https://doi.org/10.1109/TPEL.2008.2008441>.
- [2] J. He, K. Chen, M. Li, Y. Luo, C. Liang, Y. Xu, Review of Protection and Fault Handling for a Flexible DC Grid, *Prot. Control Mod. Power Syst.* 5 (2020), <https://doi.org/10.1186/s41601-020-00157-9>.
- [3] A.B. High Voltage DC Systems and the Related CommissioningHaliloglu, I. Iskender, HIGH VOLTAGE DC SYSTEMS AND THE RELATED COMMISSIONING, *Int. J. Tech. Phys. Probl. Eng.* 12 (2020) 90–98. <https://www.scopus.com/inward/record.uri?eid=2-s2.0-85083742156&partnerID=40&md5=7c65937007dd67d91498926c2f26188290A> %0ADOCUMENT TYPE: Article%0APUBLICATION STAGE: Final%0ASOURCE: Scopus.
- [4] M. Ashouri, F.F. da Silva, C.L. Bak, A pilot protection scheme for VSC-MTDC grids based on polarity comparison using a combined morphological technique, *Electr. Eng.* 104 (2022) 1395–1411, <https://doi.org/10.1007/s00202-021-01347-w>.
- [5] Z. Yao, Q. Zhang, P. Chen, Q. Zhao, Research on Fault Diagnosis for MMC-HVDC Systems, *Prot. Control Mod. Power Syst.* 1 (2016) 1–7, <https://doi.org/10.1186/s41601-016-0022-0>.
- [6] A.F. Abdou, A. Abu-Siada, H.R. Pota, Impact of VSC Faults on Dynamic Performance and Low Voltage Ride Through of DFIG, *Int. J. Electr. Power Energy Syst.* 65 (2015) 334–347, <https://doi.org/10.1016/j.ijepes.2014.10.014>.
- [7] M. Muniaappa, A Comprehensive Review of DC Fault Protection Methods in HVDC Transmission Systems, *Prot. Control Mod. Power Syst.* 6 (2021) 1–20, <https://doi.org/10.1186/s41601-020-00173-9>.
- [8] H.M. Ryan, *High-Voltage Engineering and Testing High-Voltage Engineering and Testing*, 3rd ed., The Institution of Engineering and Technology, 2013.
- [9] A.V. Mytnikov, *High voltage engineering*, Tomsk Polytechnical University (2012).
- [10] V. a Rakov, Bonding versus isolating approaches in lightning protection practice, *Light. Prot. (ICLP)*, 2008 Int. Conf. (2008) 1–11.
- [11] E. Kuffel, W.S. Zaengl, J. Kuffel, *High Voltage Engineering Fundamentals*, Second ed., Butterworth Heinemann, 2000. 10.1016/0-7506-3634-6.x5000-x.
- [12] M. Goertz, S. Wenig, S. Gorges, M. Kahl, S. Beckler, J. Christian, M. Suriyah, T. Leibfried, Lightning overvoltages in a HVDC transmission system comprising mixed overhead-cable lines, in: *Int. Conf. Power Syst. Transients*, 2017.
- [13] M. Goertz, S. Wenig, C. Hirsching, M. Kahl, M. Suriyah, T. Leibfried, Analysis of Extruded HVDC Cable Systems Exposed to Lightning Strokes, *IEEE Trans. Power Deliv.* 33 (2018) 3009–3018, <https://doi.org/10.1109/TPWRD.2018.2858569>.
- [14] C.K. Jung, J.W. Kang, K.Y. Shin, D.H. Kim, D.I. Lee, S. Korea, G.P. Office, Lightning analysis on HVDC / HVAC hybrid transmission system in Korea, in: *XVII Int. Symp. High Volt. Eng. Hann. Ger.*, 2011: pp. 1–5.
- [15] F.M.F. da Silva, K. Schultz Pedersen, C.L. Bak, Lightning in hybrid cable-overhead lines and consequent transient overvoltages, in: *Proc. IPST 2017*, 2017.
- [16] T.V. Gomes, M.A.O. Schroeder, R. Alipio, A.C.S. De Lima, A. Piantini, Investigation of Overvoltages in HV Underground Sections Caused by Direct Strokes Considering the Frequency-Dependent Characteristics of Grounding, *IEEE Trans. Electromagn. Comput.* 60 (2018) 2002–2010, <https://doi.org/10.1109/TEMC.2018.2798291>.
- [17] M. Asif, H.Y. Lee, U.A. Khan, K.H. Park, B.W. Lee, Analysis of Transient Behavior of Mixed High Voltage DC Transmission Line under Lightning Strikes, *IEEE Access.* 7 (2019) 7194–7205, <https://doi.org/10.1109/ACCESS.2018.2889828>.
- [18] O. Lennerhag, J. Lundquist, C. Engelbrecht, T. Karmokar, M.H.J. Bollen, An Improved Statistical Method for Calculating Lightning Overvoltages in HVDC Overhead Line/Cable Systems, *Energies*. 12 (2019), <https://doi.org/10.3390/en12163121>.
- [19] P. Ghosh, A.K. Das, S. Dalai, S. Chatterjee, The effects of non-standard lightning impulse on electrical insulation: a review, *Electr. Eng.* 104 (2022) 4239–4254, <https://doi.org/10.1007/s00202-022-01616-2>.
- [20] Cigre, *WGB4.63, Testing and Commissioning of VSC, HVDC Systems* (2017).
- [21] H. Saad, P. Rault, S. Denettière, Study on transient overvoltages in converter station of MMC-HVDC links, *Electr. Power Syst. Res.* 160 (2018) 397–403, <https://doi.org/10.1016/j.epdr.2018.03.017>.
- [22] Y. Han, Y. Lu, Study on the insulation coordination of ±800kV converter station in the nuozhadu to guangdong HVDC power transmission project, *Adv. Mater. Res.* 354–355 (2012) 1205–1209, <https://doi.org/10.4028/www.scientific.net/AMR.354-355.1205>.
- [23] D.J. Wang, H. Zhou, Comparison of insulation coordination between ±800kV and ±1100kV UHVDC systems, *J. Electr. Eng. Technol.* 10 (2015) 1773–1779, <https://doi.org/10.5370/JEET.2015.10.4.1773>.
- [24] Y.L. Gu, X.M. Huang, P. Qiu, W. Hua, Z.R. Zhang, Z. Xu, Study of overvoltage protection and insulation coordination for MMC based HVDC, *Appl. Mech. Mater.* 347–350 (2013) 1812–1817, <https://doi.org/10.4028/www.scientific.net/AMM.347-350.1812>.
- [25] F. Schettler, H. Huang, N. Christl, HVDC Transmission Systems using Voltage Sourced Converters - Design and Applications, in: *Power Eng. Soc. Summer Meet.*, Seattle, WA, 2000: pp. 715–720. 10.1109/PESS.2000.867439.
- [26] IEC Standard 60071-1+A2-2010, Insulation Co-ordination Part 1: Definitions, Principles and Rules, (IEC), Int. Electrotech. Comm. (2010).
- [27] A.B. Haliloglu, I. Iskender, Design Studies of VSC HVDC Converter According to AC Voltage Tests, *Energies*. 15 (2022), <https://doi.org/10.3390/en15207628>.
- [28] CIGRE Report 113 WG14.01 TFO3, Test circuit for HVDC thyristor valves, 1997.
- [29] Cigre, *WGB4.4, Components Testing of VSC System for HVDC, Applications* (2011).
- [30] M.Y. Ataka, L.L. Bacci, T.M. Lima, R.F.R. Pereira, E.C.M. Costa, L.H.B. Liboni, Lighting protection of VSC-HVDC transmission systems using ZnO surge arresters, in: *Can. Conf. Electr. Comput. Eng.*, 2020: pp. 1–5. 10.1109/CCECE47787.2020.9255785.
- [31] G.V.S. Rocha, R.P.D.S. Barradas, J.R.S. Muniz, U.H. Bezerra, I.M. De Araújo, D.D.S. A. Da Costa, A.C. Da Silva, M.V.A. Nunes, J.S.E. Silva, Optimized surge arrester allocation based on genetic algorithm and ATP simulation in electric distribution systems, *Energies*. 12 (2019), <https://doi.org/10.3390/en12214110>.
- [32] J. Kang, Comprehensive analysis of transient overvoltage phenomena for metal-oxide varistor surge arrester in LCC-HVDC transmission system with special protection scheme, *Energies*. 15 (2022), <https://doi.org/10.3390/en15197034>.

- [33] V. Vita, C.A. Christodoulou, Comparison of ANN and finite element analysis simulation software for the calculation of the electric field around metal oxide surge arresters, *Electr. Power Syst. Res.* 133 (2016) 87–92, <https://doi.org/10.1016/j.epsr.2015.11.041>.
- [34] V. Vita, A.D. Mitropoulou, L. Ekonomou, S. Panetsos, I.A. Stathopoulos, Comparison of metal-oxide surge arresters circuit models and implementation on high-voltage transmission lines of the Hellenic network, *IET Gener. Transm. Distrib.* 4 (2010) 846–853, <https://doi.org/10.1049/iet-gtd.2009.0424>.
- [35] CIGRE Report 441 WGC.4.402, Protection of Medium Voltage and Low Voltage Networks Against Lightning Part 2: Lightning protection of Medium Voltage Networks, 2010.
- [36] CIGRE Report 287 WGC4.4.02, Protection of MV and LV networks against lightning Part 1: common topics, 2006. 10.1049/cp:19970490.
- [37] J. Wang, X. Zhang, Double-exponential expression of lightning current waveforms, *Proc. - Fourth Asia-Pacific Conf. Environ. Electromagn. CEEM'2006.* (2006) 320–323. 10.1109/CEEM.2006.257962.
- [38] B. Filipović-Grčić, D. Filipović-Grčić, A new method for estimation of time parameters of standard and non-standard switching impulse voltages, *Int. J. Electr. Power Energy Syst.* 96 (2018) 126–131, <https://doi.org/10.1016/j.ijepes.2017.10.001>.
- [39] K. Hemapala, O. Swathika, K. Dharmadasa, Techno-Economic Feasibility of Lightning Protection of Overhead Transmission Line with Multi-Chamber Insulator Arrestors, *Dev. Eng.* 3 (2018) 110–116, <https://doi.org/10.1016/j.deveng.2018.05.003>.
- [40] IEC Standard 60099-5:2018, Surge arresters – Part 5: Selection and application recommendations, (IEC), Int. Electrotech. Comm. (2018) 130.
- [41] CIGRE WG01 SC33, Guide to procedures for estimating the lightning performance of transmission lines, 1991.
- [42] IEEE Std 1410-2004, IEEE guide for improving the lightning performance of electric power overhead distribution lines, (IEEE), Inst. Electr. Electron. Eng. (2004). <http://ieeexplore.ieee.org/servlet/opac?punumber=5706449>.
- [43] V.P. Larionov, Protection against lightning. Part 1, Elektrichesvo. (1999) 51–58.
- [44] IEC Standard 60099-4:2014, Surge Arresters Part 4: Metal-Oxide Surge Arresters Gaps for A.C. Systems, (IEC), Int. Electrotech. Comm. (2014).
- [45] C.K. Kim, V.K. Sood, G.S. Jang, S.J. Lim, S.J. Lee, H.V.D.C. Transmission, Power Conversion Applications in Power Systems (2010), <https://doi.org/10.1002/9780470822975>.
- [46] IEEE Std, C62.22-2009, IEEE Guide for the Application of Metal-Oxide Surge Arresters for Alternating-Current Systems, (IEEE), Inst. Electr. Electron. Eng. (2009).
- [47] IEC Standard 60099-9:2014, Surge Arresters Part 9: Metal-Oxide Surge Arresters without Gaps for HVDC Converter Stations, (IEC), Int. Electrotech. Comm. (2014).
- [48] B. Richter, Overvoltage protection - Metal-oxide surge arresters in medium-voltage systems, ABB Switz. Ltd. (2018) 60. www.abb.com/arrestersonline.
- [49] IEC Standard 60071-5-2015, Insulation Co-ordination Part 5: Procedures for High-Voltage Direct Current (HVDC) Converter Stations, (IEC), Int. Electrotech. Comm. (2015).
- [50] IEC Standard 60060-1-2010, High-Voltage Test Techniques Part 1: General Definitions and Test Requirements, (IEC), Int. Electrotech. Comm. (2010).
- [51] IEC Standard 62501-2009+A2-2017, Voltage Sourced Converter (VSC) Valves for High-Voltage Direct Current (HVDC) Power Transmission - Electrical Testing, (IEC), Int. Electrotech. Comm. (2017).
- [52] IEC Standard 60071-1:2019, Insulation Co-ordination Part 1: Definitions, Principles and Rules, (IEC), Int. Electrotech. Comm. (2019).
- [53] IEC Standard 60060-3-2006, High Voltage Test Techniques Part 3: Definitions and Requirements for On-Site Tests, (IEC), Int. Electrotech. Comm. (2006).